Journal of Materials Chemistry B

Accepted Manuscript

ROYAL SOCIETY OF CHEMISTRY

www.rsc.org/materialsB

3-D Scaffold Platform for Optimized Non-viral Transfection of Multipotent Stem Cells

Xiaohua Yu[1], W. L.Murphy[1,2,3,4*]

Affiliations:
1. Department of Biomedical Engineering, University of Wisconsin, Madison, WI 53706, USA
2. Materials Science Program, University of Wisconsin, Madison, WI 53706, USA
3. Department of Orthopedics and Rehabilitation, University of Wisconsin, Madison, WI 53705, USA
4. AO Foundation Collaborative Research Center, Davos, Switzerland

*To whom correspondence should be addressed.
William L. Murphy, Ph. D
Department of Biomedical Engineering
University of Wisconsin
1111 Highland Ave
Madison, WI 53705
Tel.: + 1 608 262 2224
Fax: + 1 608 265 9239
E-mail address: wlmurphy@wisc.edu (W.L. Murphy)

Abstract

Optimization of non-viral gene delivery from biomaterials is of critical importance, as several material parameters are known to influence non-viral transfection efficiency. A series of previous studies have achieved screening of gene delivery vectors on two dimensional (2D) substrates, which have direct relevance to cell culture applications. There is an additional need to create screening systems that are 3-dimensional (3D), and can thus be applied to emerging tissue engineering applications. Here, we report an enhanced throughput, 3D scaffold platform to screen for the influence of mineral coating properties on stem cell transfection. Mineral coatings with a range of physicochemical properties were formed on the scaffolds within a 96-well plate format, while maintaining an interconnected macroporous scaffold structure. A series of general gene delivery parameters, including plasmid amount, N/P ratio, and cell density, were efficiently screened in scaffolds using a luciferase-encoding plasmid as a reporter. In addition, human mesenchymal stem cell (hMSC) transfection with a plasmid encoding bone morphogenetic protein-2 (BMP-2) was successfully optimized by screening a library of mineral coatings, resulting in over 5-fold increases in BMP-2 production when compared to standard techniques. Notably, the majority of BMP-2 was incorporated into the mineral coating following secretion from the cells. The 3D mineral coated scaffold platform described here may accelerate gene delivery optimization and improve the predictability of the screening systems, which could facilitate translation of gene delivery to clinical applications.

1 Introduction

Gene delivery has been extensively explored in the last few decades in order to effectively transfer genetic material into specific cells[1–3]. Non-viral gene delivery systems have attracted considerable interest recently due to their desirable safety profile, low immune response, and ease of synthesis, but their clinical applications have been limited by their low transfection efficiency when compared to viral vectors[4]. Optimization of various parameters, such as transfection reagent, DNA/reagent ratio, and medium for complexation can significantly improve non-viral gene delivery efficiency[5]. Indeed, it was reported that up to a 1000-fold increase in transfection efficiency could be achieved by simply changing the transfection parameters[6]. In view of the potential to increase transfection efficiency, several recent studies have described screening systems to efficiently optimize transfection parameters, such as condensing reagents, cell type/density, and substrate nanotopography[7–9]. For example, Lynn et al. screened 140 biodegradable cationic polymers in a combinatorial format and identified the ones suitable for DNA condensation[10]. While these screening approaches have identified conditions and reagents of substantial interest and direct relevance to cell culture applications, they may not correlate ideally to gene delivery from 3-dimensional (3D) scaffolds for tissue engineering applications. Most of current gene delivery screenings were performed on two dimensional (2D) monolayer cell culture, in which the gene to be delivered have almost unlimited access to the target cells[11]. On the other hand, cells grown in 3D culture systems such as tissue engineering scaffolds had limited access to the target gene/complex due to various barriers (complex size, diffusion, and gradient)[12]. These challenges associated with gene delivery in 3D culture have motivated us to develop a 3D screening system to optimize gene delivery in the context of 3D cell culture and tissue engineering. Besides, the optimal transfection condition identified on 3D scaffolds can be directly translated into gene delivery-based therapeutics whereas 2D screenings can only be regarded as screening tools. ~~Compared to cells grown on 2D, cells in three dimensional (3D) scaffolds can exhibit substantially different cell morphology, adhesion, and proliferation, and these cellular behaviors could influence gene delivery efficiency[13,14]. Therefore, non-viral gene delivery screening systems in 3D scaffold formats are desirable for 3-D cell culture *in vitro* and tissue engineering *in vivo* applications.~~

Previous studies have demonstrated optimization of non-viral transfection via organic materials (e.g. synthetic polycations, peptides, and cationic lipids)[8,10,15]. Here we focus on identifying optimal inorganic materials, particularly calcium phosphate (CaP) mineral coatings. CaP based mineral coatings have been applied to various biomaterials surface via a "biomimetic" approach, in which mineral coatings are formed by incubating in modified simulated body fluid (mSBF) [16–18]. Mineral coatings formed in this manner have been shown to improve physicochemical and biological properties upon their formation on biomaterials[19,20], and they have also demonstrated their potential to be used as carriers for gene delivery[21,22]. For example, co-precipitation of DNA with mineral coating on a 2D substrate resulted in increased gene transfer efficiency and sustained gene expression[23]. Furthermore, several recent studies from our group and others have shown that intrinsic properties of mineral coatings serve as important factors for controlling gene transfer efficiency[24–26]. However, there is a broad range of relevant mineral properties (e.g. solubility, morphology, crystallinity, composition, porosity, DNA binding affinity), and the

influence of these properties on gene transfer has not been explored in the context of 3-D tissue engineering scaffolds. Thus, there is a need for high throughput experimental formats that systematically vary the properties of mineral coatings to optimize gene delivery to resident cells.

Here we report an enhanced throughput, 3D scaffold platform to screen for the influence of CaP mineral coating properties on human stem cell transfection. 3D poly (lactide-co-glycolide) (PLG) scaffolds were fabricated in a 96-well plate format to enable efficient screening. Mineral coatings were then formed on the scaffolds within the wells, while systematically varying the coating conditions from well-to-well. We hypothesized that systematic changes in mSBF composition would result in corresponding changes in mineral coating properties, which would then lead to distinct gene transfer efficiencies. Our results indicate that stem cell transfection was efficiently optimized using our 3D mineral coated scaffold platform. The enhanced throughput screening system demonstrated here might trigger the development of gene delivery devices that can be translated to an *in vivo* context for tissue engineering applications.

2 Materials and methods

2.1 Fabrication of 3D scaffold arrays in96-well plates

Poly (lactide-co-glycolide) (PLG) 3D scaffold arrays were fabricated using a salt fusion/solvent casting/salt leaching technique in 96-well plates. Briefly, 130-135 mg of sieved NaCl particles (250 µm-450 µm) were added into each well and subjected to 95% humidity at 37°C for 4 h to achieve fusion of NaCl crystals. Then the fused salt template was dried in an oven at 50°C for 2 h. 30 µL of 10% PLG (Sigma-Aldrich, St Louis, MO) in acetone was added onto the salt template in each well and the whole plate was centrifuged at 2000 RPM for 2 min to wet all the NaCl particles. The plate with scaffolds was placed in fume hood at room temperature to evaporate the solvent overnight. The whole plate was then immersed in 4.0 L beaker filled with DI water to leach the NaCl out. The water was refreshed every 4 h and the leaching process took approximately 48 h (Fig. 1-A).

2.2 Formation and characterization of mineral coating

PLG scaffolds in 96-well plates were first treated with 0.1 M NaOH for 5 min and rinsed with DI water. For mineral formation, a series of modified simulated body fluids (mSBFs) were prepared by dissolving 141.0 mM NaCl, 4.0 mM KCl, 0.5 mM $MgSO_4$, 1.0 mM $MgCl_2$, $NaHCO_3$ (Table 1), $CaCl_2$ (Table 1), KH_2PO_4 (Table 1), and 20 mM MES buffer (Fisher Scientific, Pittsburgh, PA) in DI water as described in our previous study[24]. 200 µL of 10× mSBF was added into each well and incubated overnight to rapidly form a "precursor" mineral coating. After extensively washing with DI water, various mSBFs were added to scaffolds at 37 ºC for 7 days with twice mSBF refreshment daily to grow additional coatings upon the precursor coating. The resulting mineral coated scaffolds in 96-well plates were then rinsed in DI water and air dried for mineral coating characterization (Fig. 1-A). To confirm the formation of mineral coatings on PLG scaffolds, representative scaffolds were removed from the 96-wells and subjected to scanning electron microscopy (SEM) examination after sputter-coating with gold. The uniformity of mineral coating on PLG scaffolds was also visualized by Alizarin red S (Sigma-Aldrich, St Louis, MO) staining to identify calcium deposition.

2.3 Cell culture

C3H10T1/2 cells were cultured in Dulbecco's Modified Eagle Medium (DMEM) (Mediatech, Manassas, VA) supplemented with 10% cosmic calf serum (CCS) and 1% penicillin/streptomycin (PS) on flask at 37 ºC and 5% CO_2. Human mesenchymal stem cells (hMSCs) were grown on flask in α-Modified Eagle Medium (α-MEM) (Mediatech, Manassas, VA) supplemented with 10% fetal bovine serum (FBS) and 1% PS. Upon sub-confluence, both types of cells were harvested from the flasks with 0.05% trypsin-EDTA and re-suspended for seeding on scaffolds.

2.4 Transfection optimization on 3D scaffold array

pMetLuc reporter plasmid (pLuc) (Clontech, Mount View, CA) was amplified using competent TOF10F' E. coli (Life Technologies, Carlsbad, CA) and purified using a Giga plasmid purification kit (Qiagen, Valencia, CA) following the protocol from the manufacture. pLuc lipoplexes were formed by mixing Lipofectamine2000 (Life Technologies, Carlsbad, CA) with pLuc at various N/P ratio (0.5/1/2/3) using Opti-MEM® medium. pLuc amounts loaded into each well were varied (0.5/1/2/5 µg per well) to optimize the cell transfection on the scaffold arrays. Mineral coated scaffolds were incubated in 100 µL Opti-MEM® containing various amounts of pLuc complexes for 2 h to allow the adsorption of the complexes within the mineral coatings. The unbound pLuc complexes were removed by washing with 200 µL Opti-MEM® before transfection. At the time of transfection, collected C3H10T1/2 cells were seeded onto the scaffolds. For scaffolds loaded with 1.0 µg/well pLuc at N/P=2, cell seeding densities were varied from 25,000 to 200,000 cells/well. For other tested transfection parameters, 100,000 cells were seeded into each well. After 48 h of culture, cell culture medium was collected from each well. Luciferase activity was measured using a Cell-Glow Luciferase assay kit (Clontech, Mountain View, CA). The luminescence was measured by a Bio-Rad microplate reader (Bio-Rad, PA) set with a bioluminescence mode. In addition, luminescence per well was imaged with an In Vivo Imaging System (IVIS, Caliper Life Science, Mountain View, Ca). Cell metabolic activity in each well after transfection was evaluated by the CellTiter-Blue assay kit (Promega, Madison, WI).

2.5 Screening BMP-2 production using mineral coated scaffold arrays

BMP-2 plasmid (pcDNA3.1/His/hBMP-2) (pBMP-2) was a gift from Prof. J. Alblas (Utrecht University, the Netherlands). pBMP-2 was mixed with Lipo2000 at N/P ratio of 2 in Opti-MEM® reduced serum medium and loaded onto mineral coated scaffold at 1.0 µg/well. After 2 h incubation at 37 ºC, the binding efficiency of pBMP-2 on the scaffolds was determined by measuring the remaining pBMP-2 in the supernatant using a PicoGreen assay (Life Technology, Carlsbad, CA). After washing the scaffolds with Opti-MEM® reduced serum medium, 100,000 hMSCs were seeded onto the mineral coated scaffold in each well. The supernatant was collected from each well after 72 h of culture. Then, 100 µL 100 mM EDTA/PBS (pH=7.4) was added into each well and incubated at 37 ºC for 15 min to dissolve the mineral coating. The supernatant was collected after centrifuged at 11,000 RPM for 2 min. BMP-2 expression was determined in both cell culture medium and mineral dissolved solution using a BMP-2 Quantikine ELISA Kit (R&D Systems, MN) following the manufacture instructions.

2.6 Statistical analysis

Quantitative data are expressed as mean ± standard deviation. Statistical analysis was performed for all quantitative data using a one-way analysis of variance (one-way ANOVA). p value < 0.05 is considered as a statistically significant difference.

3 Results and discussion

3.1 Establishment of mineral coated 3D scaffold array

We first established a 3D mineral coated scaffold array in a 96-well plate to identify optimal coating properties for non-viral transfection of multipotent stem cells. This approach successfully combined the fabrication of tissue engineering scaffolds and formation of mineral coatings on each scaffold's surface in an enhanced throughput manner for efficient screening. PLG was selected as the starting material for scaffold array fabrication since it is one of the most representative synthetic polymers used for various biomedical applications including medical device, tissue engineering and drug delivery. As shown in Fig. 1-B, a PLG scaffold was obtained in each well of a 96-well plate after a salt fusion, solvent casting, and salt leaching process described previously[27]. The gross appearance of the scaffold exhibited a homogeneous structure with numerous interconnected macropores observed throughout the scaffold (Fig. 1-C). SEM micrographs revealed that the scaffolds were highly porous, with pore size between 200-400 μm in diameter. The macropores appeared to be interconnected by numerous smaller pores (Fig.1-E) and the uniformly distributed macropores were found throughout the whole scaffold thickness (Fig. S-1-E). Scaffold properties were consistent with prior results in larger scale formats, in which the same salt fusion technique was used to ensure an interconnected pore structure[27].

The 3D scaffold array was then coated with mineral by incubating in mSBF, and the formation of the mineral coating was confirmed by both Alizarin Red S staining and SEM (Fig. 1-D&F). The strong staining covering the majority of the scaffold indicated abundant calcium deposition on the scaffold. SEM images showed a layer of mineral covering the scaffold, and also showed that the mineral coating did not significantly change the pore size. This result is not surprising, as the thin mineral coatings formed using mSBF incubation have typically had thickness on the order of 10 μm, which would not significantly influence a 200-400 μm initial pore size. The mineral coating also grew throughout the thickness of the 3D scaffolds, as shown in Fig. 1-G. The success of mineral coating formation on PLG scaffolds could be attributed to ~~two~~ three factors. First, alkaline treatment for surface hydrolysis of the scaffold prior to incubation in mSBF may have facilitated mineral nucleation by exposing more hydroxyl and carboxyl groups[28,29]. Second, the utilization of 10X mSBF greatly improved the uniformity of mineral coating on scaffold compared with the scaffolds without this treatment (Fig. S-1). Third, the salt fusion technique substantially improves the interconnectivity of the macroporous scaffolds (Fig. 1-E), and may have improved transport of mSBF-borne mineral ions into the scaffolds[27].

Previous studies from our group on 2-D mineral coatings have shown that subtle changes in mineral coating properties led to substantial variations in non-viral transfection[24]. We further expanded this concept here by systematically varying coating properties in the 3D scaffolds. Specifically, we exploited the well-plate format to systemically vary the ion concentrations in mSBF in order to tune the properties of mineral coatings. [Ca^{2+}], [PO_4^{3-}], and [CO_3^{2-}] were varied

in the mSBF, as these ions have prominent roles during coating nucleation and growth[30]. SEM at low magnification showed continuous mineral coatings within PLG scaffolds in 96-well plates in each condition, regardless of changes in mSBF contents (Fig. 2-Low Mag). The macroporous structures were maintained in all the mSBF conditions tested, indicating that coatings would not likely impair cell seeding or infiltration in subsequent studies. The changes in coating morphology caused by varying mSBF content were observed in higher magnification SEM images (Fig. 2-High Mag). Increases in $[CO_3^{2-}]$ from 4.2 mM to 100 mM resulted in a transformation of the plate-like coating structure from micrometer scale porosity to nanometer scale porosity. The effect of increasing $[CO_3^{2-}]$ on coating morphology was less apparent in conditions with higher $[Ca^{2+}]$ and $[PO_4^{3-}]$ (3.5× and 5× relative to standard mSBF concentrations). Taken together, these data indicated an ability to vary mineral coating properties in 3-D scaffolds in an efficient, 96-well format.

3.2 Optimization of non-viral gene delivery in mineral coated 3D scaffold arrays

We next evaluated the effectiveness of the 3D mineral coated scaffold arrays for optimized non-viral transfection, using a plasmid encoding the reporter protein luciferase (pLuc). The PLG scaffolds in 96-well plates were first coated uniformly with mineral generated in standard 2× mSBF. The pLuc was firstly condensed using Lipofectamine2000 to form complex, and incorporated onto the mineral coatings via electrostatic interactions[24]. Compared with cells on PLG scaffold transfected with standard protocol, the transfection efficiency of mineral coated PLG scaffold increased over 100% in term of luciferase activity (Fig. 3-A), which suggests our approach was superior than conventional solution based transfection method. In order to screen for common transfection parameters, including pLuc amount, N/P ratio (using Lipofectamine 2000 as the condensing agent), and cell seeding density,12 different conditions were screened with three replicates for each condition, which used only 36 wells of a 96-well plate (Fig. 3-B). Results showed that increasing pLuc amount above 1 μg/well resulted in decreasing luciferase activity, which might be caused by cytotoxicity at these high dosages of pLuc/Lipo2000 (Fig. 3-C&D). The highest luciferase activity was detected when the N/P ratio was set at 2. The variation in N/P ratio between 0.5-3 did not cause significant cytotoxicity, as the cell viability was not dependent on N/P ratio in this range (Fig. 3-E&F). Cell density had an impact on cell viability, but did not substantially influence expression of the pLuc transgene (Fig. 3-G&H). The higher cytotoxicity in low cell density groups might be due to the relatively higher pLuc/Lipo2000 complex availability for each cell as fewer cells were exposed to the same amount of complex compared with high cell density conditions. Collectively, these data demonstrate the ability to use an array of mineral coated scaffolds to efficiently screen for parameters that influence cell viability and non-viral transfection, and to identify "hit" conditions to be used in subsequent studies.

Notably, the format described here contrasts with most *in vitro* screening systems developed to date, which grow cells as monolayers on 2D substrates. This distinction is important, as some intended applications of cell transfection involve tissue engineering applications that are inherently 3D, and cells also reside in 3D extracellular matrices (ECMs) *in vivo*[31]. One critical issue for non-viral gene delivery is that many 2D gene delivery strategies cannot be translated into 3D systems such as scaffolds, hydrogels and other formats[32]. Even high transfection efficiency are achieved in 2D culture with tranfection reagents such as Lipofectamine, PEI, and

PLL, these techniques cannot be used for therapeutic purpose if they cannot be applied on 3D systems[33,34]. The conversion from 2D to 3D system is realized by the incorporation of DNA complex onto mineral coating formed on 3D scaffolds. Furthermore, traditional 3D approaches evaluate scaffolds one at a time, which is not a suitable approach for high throughput screening and optimization of transfection[35]. The 96-well scaffold array we describe here addresses these issues, as up to 96 scaffolds can be generated and tested simultaneously. Importantly, the cells grow in a 3D scaffold, which may allow them to represent with greater predictability their behavior upon implantation *in vivo*.

3.3 Screening of BMP-2 expression using mineral coated 3D scaffold arrays

A series of pre-clinical and clinical studies have demonstrated that bone morphogenetic protein-2 (BMP-2) can induce bone formation in multiple *in vivo* contexts[36,37]. Thus, there has been substantial interest in delivering genes encoding BMP-2 in bone tissue engineering applications[38–40]. In view of this potential application, we chose to screen for the effects of coating properties on non-viral delivery of a plasmid encoding BMP-2 (pBMP-2). We hypothesized that by systematically changing mineral coating properties, distinct BMP-2 expression levels would be achieved. A condensed pBMP-2/Lipo2000 complex was incorporated into mineral-coated scaffolds via a 2 h soaking process. The pBMP-2 complex incorporation efficiencies showed only minor differences between different mineral coatings, despite the significant differences in coating properties (Fig. 4-A). hMSCs were then seeded onto pBMP-2 loaded, mineral-coated scaffolds and evaluated for BMP-2 production during a 72 h incubation. BMP-2 production was detected in all mineral-coated PLG scaffold conditions (Fig. 4-B). The total BMP-2 production by cells in 3D scaffolds ranged from 109-604 pg/mL, and the highest level of BMP-2 production was found on scaffolds coated with 3.5× mSBF with $[CO_3^{2-}]$ = 50 mM. Importantly, five different mineral-coated scaffold conditions were identified as "hits", as they showed higher BMP-2 production than control conditions in which pBMP-2/Lipo2000 condensates were added to hMSC cultures in solution as per manufacturer's protocol. Compared with 2D mineral coating in our previous study, 3D mineral coating on the scaffold demonstrated distinct transgene performance, which supported that 3D structure of the scaffolds could influence transgene expression. For instance, we found transfection efficiencies were closely related to carbonate substitution in the coating in our previous 2D study[24]. However, the relationship between transfection efficiency and carbonate concentration became diverging in the current 3D study. Especially, the optimal transfection condition did not correspond with the highest carbonate concentration as we showed in 2D study.

We also characterized the amount of BMP-2 present in the cell culture medium and the amount present within the mineral coatings. We hypothesized that due to the well-known affinity of the BMP-2 protein for CaP mineral coatings[41], a significant amount of the BMP-2 secreted by hMSCs would incorporate within the mineral coatings via affinity binding. Remarkably, our results indicated that the majority of the BMP-2 was present in the coating (versus in the cell culture medium) for all conditions tested. In a subset of conditions, over 80% of the BMP-2 produced by hMSCs was incorporated into the coatings (Fig. 4-C&D). This result is intriguing, as the BMP-2 incorporated into the mineral coatings is likely to serve as a reservoir for sustained BMP-2 release. This assertion is based on numerous prior studies from our group showing that proteins (including recombinant human BMP-2) incorporated into CaP mineral coatings can be

released over extended timeframes during mineral dissolution, while maintaining high levels of biological activity[42]. More specifically, we have used mineral coatings similar to those used in the current study as carriers for controllable release of BMP-2, VEGF and bFGF[43–46]. Our previous studies found that recombinant human growth factors added in solution could incorporate into mineral coatings with high efficiency(up to 60%)[44], and that the mineral coatings were able to stabilize proteins against denaturation during long term culture (data not shown). Therefore, the "trapping" of cell-secreted BMP-2 within the mineral coatings observed in the current study might not only transform the scaffold into a BMP-2 releasing depot, but also prolong the bioactivity of BMP-2.

4 Conclusions

Screening systems that can identify optimal conditions for non-viral transfection within 3-D scaffolds may lead to a variety of applications in tissue engineering. Here we developed an enhanced throughput, 3D screening system to evaluate the influence of CaP mineral coating properties on stem cell transfection. Mineral coatings with a range of physicochemical properties were formed on the scaffolds in a 96-well plate format, while maintaining an interconnected macroporous scaffold structure. An initial study using a luciferase-encoding plasmid as a reporter demonstrated our ability to screen for general parameters involved in non-viral gene delivery, including plasmid amount, N/P ratio, and cell density. In addition, hMSC transfection with a plasmid encoding bone morphogenetic protein-2 (BMP-2) was successfully optimized by screening a library of mineral coatings, resulting in production of over 600 pg/ml of BMP-2 over a 72 hour timeframe. Interestingly, the majority of the cell-secreted BMP-2 was incorporated into the mineral coating, which could then potentially serve as a depot for extended release of BMP-2. Taken together, this 3D mineral coated scaffold platform may be useful to optimize gene delivery with a broad range of plasmids and target cells, which could ultimately identify suitable scaffolds for tissue engineering applications.

Acknowledgement

The authors acknowledge financial support from the AO Foundation (Exploratory Research Grant), the National Institutes of Health (RO1AR059916), and the National Science Foundation (DMR 1105591). We would like to thank Prof. J. Alblas from Utrecht University, the Netherlands for generously providing the BMP-2 plasmid.

References

1. D. Luo and W. M. Saltzman, *Nat Biotech*, 2000, **18**, 33–37.

2. H. Storrie and D. J. Mooney, *Adv. Drug Deliv. Rev.*, 2006, **58**, 500–14.

3. J.-H. Jang, T. L. Houchin, and L. D. Shea, *Expert Rev. Med. Devices*, 2004, **1**, 127–38.

4. C. W. Pouton and L. W. Seymour, *Adv. Drug Deliv. Rev.*, 2001, **46**, 187–203.

5. E. V. B. van Gaal, R. van Eijk, R. S. Oosting, R. J. Kok, W. E. Hennink, D. J. A. Crommelin, and E. Mastrobattista, *J. Control. Release*, 2011, **154**, 218–232.

6. O. Boussif, M. A. Zanta, and J. P. Behr, *Gene Ther.*, 1996, **3**, 1074–80.

7. A. F. Adler, A. T. Speidel, N. Christoforou, K. Kolind, M. Foss, and K. W. Leong, *Biomaterials*, 2011, **32**, 3611–3619.

8. M. de Raad, E. a Teunissen, D. Lelieveld, D. a Egan, and E. Mastrobattista, *J. Control. release*, 2012, **158**, 433–42.

9. B. Sun, K. K. Tran, and H. Shen, *Biomaterials*, 2009, **30**, 6386–6393.

10. D. M. Lynn, D. G. Anderson, D. Putnam, and R. Langer, *J. Am. Chem. Soc.*, 2001, **123**, 8155–6.

11. L. De Laporte, A. L. Yan, and L. D. Shea, *Biomaterials*, 2009, **30**, 2361–2368.

12. C. X. He, Y. Tabata, and J. Q. Gao, *Int. J. Pharm.*, 2010, **386**, 232–242.

13. E. Cukierman, R. Pankov, D. R. Stevens, and K. M. Yamada, *Science*, 2001, **294**, 1708–12.

14. L. Jongpaiboonkit, W. J. King, G. E. Lyons, A. L. Paguirigan, J. W. Warrick, D. J. Beebe, and W. L. Murphy, *Biomaterials*, 2008, **29**, 3346–3356.

15. B. Martin, M. Sainlos, A. Aissaoui, N. Oudrhiri, M. Hauchecorne, J.-P. Vigneron, J.-M. Lehn, and P. Lehn, *Curr. Pharm. Des.*, 2005, **11**, 375–94.

16. X. Yu and M. Wei, *J. Biomed. Mater. Res. Part B Appl. Biomater.*, 2011, **97B**, 345–354.

17. L. Jongpaiboonkit, T. Franklin-Ford, and W. L. Murphy, *Adv. Mater.*, 2009, **21**, 1960–1963.

18. H. M. Kim, T. Himeno, M. Kawashita, T. Kokubo, and T. Nakamura, *J. R. Soc. Interface*, 2004, **1**, 17–22.

19. J. Wang, P. Layrolle, M. Stigter, and K. de Groot, *Biomaterials*, 2004, **25**, 583–592.

20. Z. Xia, X. Yu, and M. Wei*, *J. Biomed. Mater. Res. Part B Appl. Biomater.*, 2012, **100B**, 871–881.

21. A. Oyane, H. Tsurushima, and A. Ito, *J. Gene Med.*, 2010, **12**, 194–206.

22. B. Sun, M. Yi, C. C. Yacoob, H. T. Nguyen, and H. Shen, *Acta Biomater*, 2012, **8**, 1109–1116.

23. Y. Yazaki, A. Oyane, Y. Sogo, A. Ito, A. Yamazaki, and H. Tsurushima, *Biomaterials*, 2011, **32**, 4896–4902.

24. S. Choi, X. Yu, L. Jongpaiboonkit, S. J. Hollister, and W. L. Murphy, *Sci. Rep.*, 2013, **3**, 1567.

25. S. Choi and W. L. Murphy, *Acta Biomater*, 2010, **6**, 3426–3435.

26. A. Oyane, H. Tsurushima, and A. Ito, *Gene Ther.*, 2007, **14**, 1750–1753.

27. W. L. Murphy, R. G. Dennis, J. L. Kileny, and D. J. Mooney, *Tissue Eng.*, 2002, **8**, 43–52.

28. T. Kokubo, *Acta Mater.*, 1998, **46**, 2519–2527.

29. X. Yu, H. Qu, D. Knecht, and M. Wei, *J. Mater. Sci. Mater. Med.*, 2009, **20**, 287–294.

30. W. L. Murphy and D. J. Mooney, *J Am Chem Soc*, 2002, **124**, 1910–1917.

31. F. Pampaloni, E. G. Reynaud, and E. H. K. Stelzer, *Nat. Rev. Mol. Cell Biol.*, 2007, **8**, 839–45.

32. H. Hosseinkhani, T. Azzam, H. Kobayashi, Y. Hiraoka, H. Shimokawa, A. J. Domb, and Y. Tabata, *Biomaterials*, 2006, **27**, 4269–4278.

33. B. Dalby, S. Cates, A. Harris, E. C. Ohki, M. L. Tilkins, P. J. Price, and V. C. Ciccarone, *Methods*, 2004, **33**, 95–103.

34. H. Hosseinkhani, Y. Inatsugu, Y. Hiraoka, S. Inoue, H. Shimokawa, and Y. Tabata, *Tissue Eng.*, 2005, **11**, 1459–1475.

35. C. G. Simon and S. Lin-Gibson, *Adv. Mater.*, 2011, **23**, 369–387.

36. K. W.-H. Lo, B. D. Ulery, K. M. Ashe, and C. T. Laurencin, *Adv. Drug Deliv. Rev.*, 2012, **64**, 1277–91.

37. H. Schmoekel, J. C. Schense, F. E. Weber, K. W. Gratz, D. Gnagi, R. Muller, and J. A. Hubbell, *J Orthop Res*, 2004, **22**, 376–381.

38. F. Liu, R. M. Porter, J. Wells, V. Glatt, C. Pilapil, and C. H. Evans, *J. Orthop. Res.*, 2012, **30**, 1095–1102.

39. I. Ono, T. Yamashita, H.-Y. Jin, Y. Ito, H. Hamada, Y. Akasaka, M. Nakasu, T. Ogawa, and K. Jimbow, *Biomaterials*, 2004, **25**, 4709–4718.

40. H. Nie and C.-H. Wang, *J. Control. Release*, 2007, **120**, 111–121.

41. Y. Liu, R. O. Huse, K. de Groot, D. Buser, and E. B. Hunziker, *J Dent Res*, 2007, **86**, 84–89.

42. T. H. Schmidt-Schultz and M. Schultz, *Am. J. Phys. Anthropol.*, 2004, **123**, 30–9.

43. M.-P. Ginebra, C. Canal, M. Espanol, D. Pastorino, and E. B. Montufar, *Adv. Drug Deliv. Rev.*, 2012, **64**, 1090–110.

44. X. Yu, A. Khalil, P. N. Dang, E. Alsberg, and W. L. Murphy, *Adv. Funct. Mater.*, 2014, DOI: 10.1002/adfm.201302859.

45. D. Suárez-González, J. S. Lee, S. K. Lan Levengood, R. Vanderby, and W. L. Murphy, *Acta Biomater.*, 2012, **8**, 1117–24.

46. D. Suárez-González, K. Barnhart, F. Migneco, C. Flanagan, S. J. Hollister, and W. L. Murphy, *Biomaterials*, 2012, **33**, 713–721.

Figures and table caption

Table 1. Ion concentrations for CO_3^{2-} effect on mineral properties.

$\frac{[Ca^{2+}]\&[PO_4^{3-}]}{[Ca^{2+}]\&[PO_4^{3-}]_{in\ plasma}}$	2 ×				3.5 ×				5 ×			
Ca^{2+} (mM)	5	5	5	5	8.8	8.8	8.8	8.8	12.5	12.5	12.5	12.5
PO_4^{3-} (mM)	2	2	2	2	3.5	3.5	3.5	3.5	5	5	5	5
CO_3^{2-} (mM)	4.2	25	50	100	4.2	25	50	100	4.2	25	50	100
pH	6.8	6.8	6.8	6.8	6.1	6.1	6.1	6.1	5.8	5.8	5.8	5.8

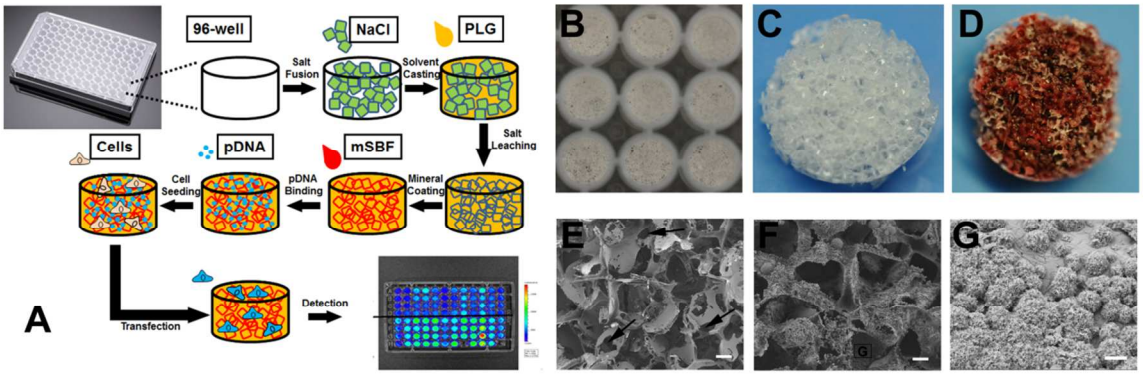

Fig 1 Non-viral gene delivery screening system using 3D mineral coated PLG scaffolds: (A) Strategy for non-viral transfection screening with enhanced throughput using a 96-well plate: PLG scaffolds were fabricated within 96-well plates and mineral coated using mSBF. Then pDNA complexes were incorporated within mineral coatings in a simple soaking process and cells were seeded onto the scaffold. Transfection was evaluated using various techniques (e.g. bioluminescence). (B) Gross appearance of PLG scaffolds in wells of a 96-well plate. (C) Gross appearance of one PLG scaffold before mineral coating formation. (D) Photograph of a mineral coated PLG scaffold stained with Alizarin Red. (E) SEM micrograph of a PLG scaffold before mineral coating (Scale bars, 100 µm) (F) SEM micrograph of a PLG scaffold after mineral coating (Scale bars, 100 µm) (G) Higher magnification SEM micrograph of a mineral coating formed on a PLG scaffold (Scale bars, 5 µm)

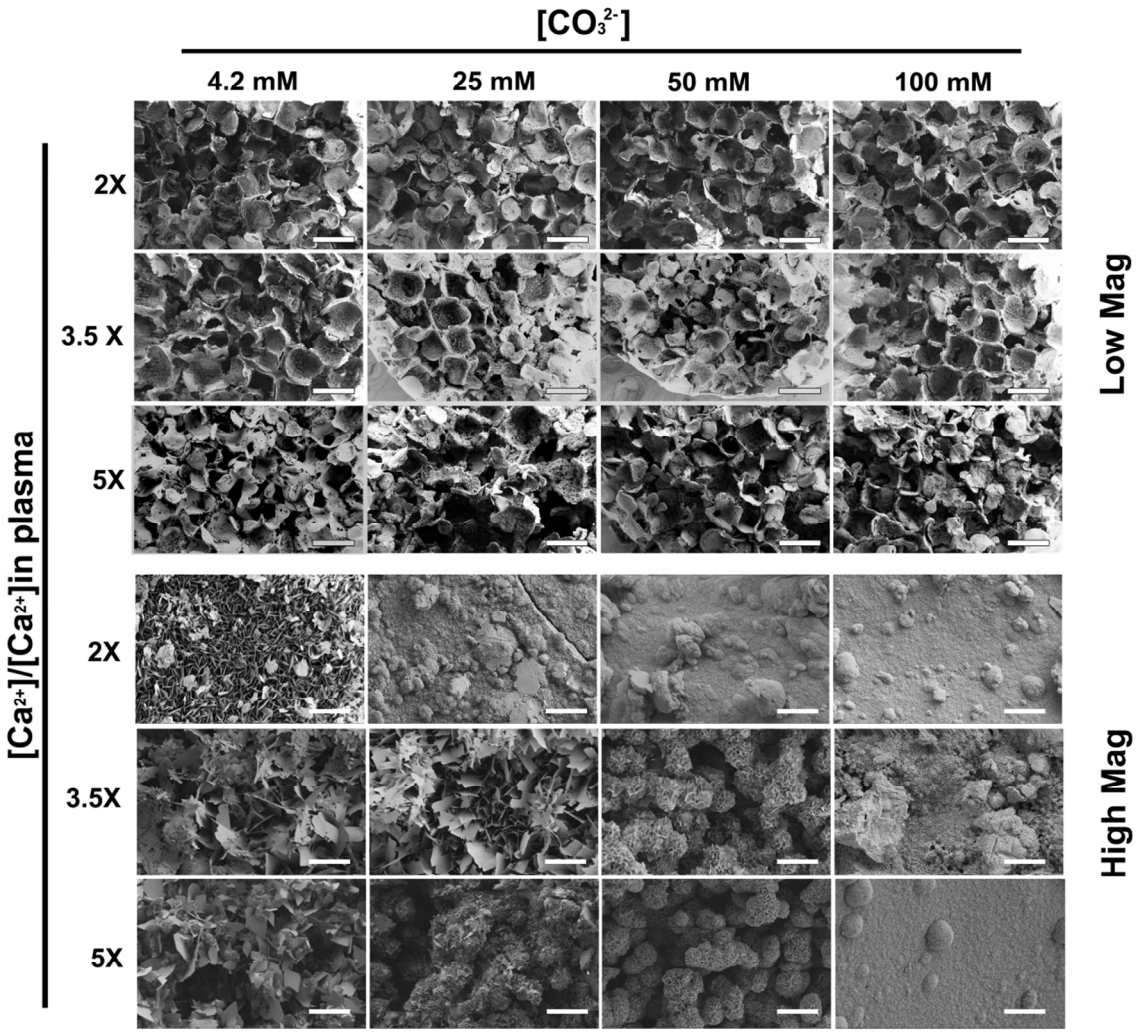

Fig 2 SEM micrographs of mineral coated PLG scaffolds in a 96-well plate: mineral coatings were formed by incubating in mSBF solutions contain various [Ca^{2+}], [PO_4^{3-}], and [CO_3^{2-}]. Low Mag images show no significant influence of mineral coating formation on the macroscopic structure of PLG scaffolds (Scale bars, 500 μm). High Mag shows the morphology of mineral coatings, which is significantly influenced by the characteristics of the mSBF, and can be readily varied (Scale bars, 5 μm)

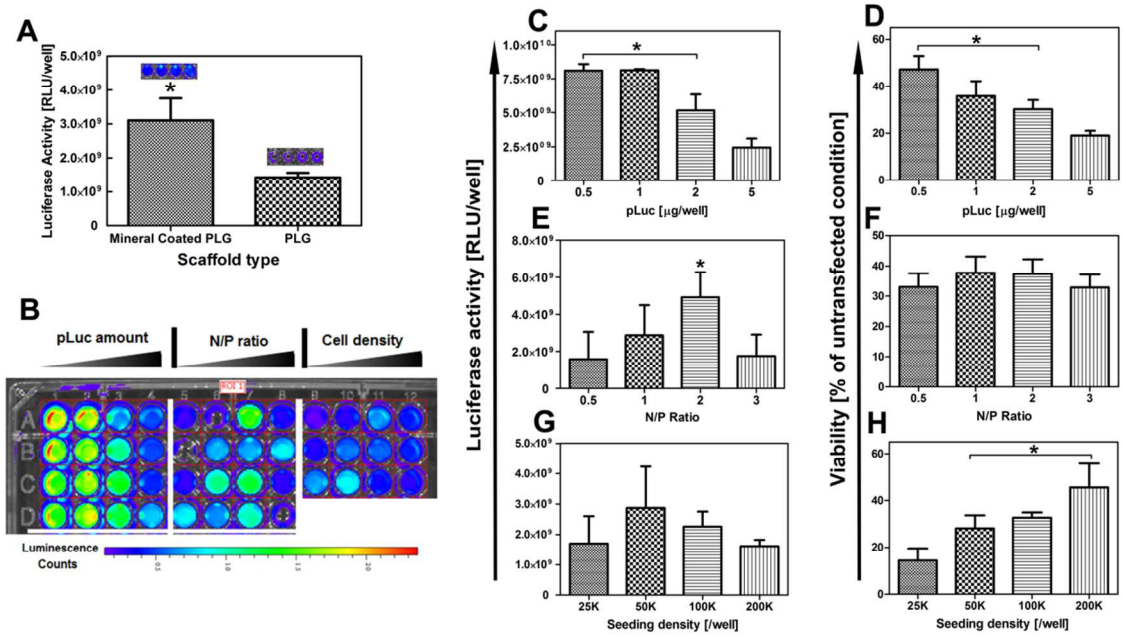

Fig 3 Screening of general parameters for stem cell transfection using 3D mineral coated PLG scaffolds. Mineral coatings were formed in 2×mSBF with 4.2 mM CO_3^{2-}. (A) Comparison of luciferase activity between PLG and mineral coated PLG scaffold with different transfection approaches. (B) Luminescence intensity from cell culture medium after 2 day culture of C3H10T1/2 cells under various transfection conditions. (C) The influence of pLuc complex amount on Luciferase activity, * indicates significant difference compared to loading amount at 5 μg/well (D) The influence of pLuc complex amount on cell viability, * indicates significant difference compared to loading amount at 5 μg/well (E) The influence of N/P ratio on luciferase activity, * indicates significant difference compared to all other N/P ratios (F) The influence of N/P ratio on cell viability. (G) The influence of cell seeding density on luciferase activity. (H) The influence of cell seeding density on cell viability, * indicates significant difference compared to seeding density at 25K/well

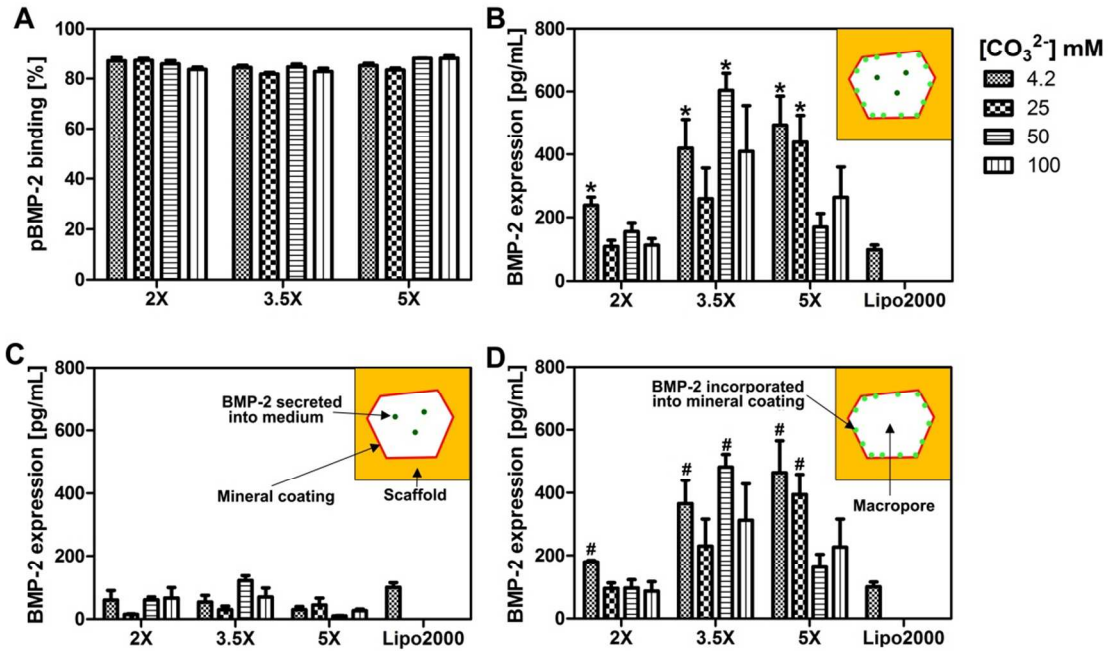

Fig 4 Screening of optimal BMP-2 expression by hMSCs using 3D mineral coated scaffolds: (A) pBMP-2 complexes binding on mineral coatings. The binding of the complexes was measured after 2 h incubation on the mineral coated scaffolds. (B) Total amount of BMP-2 produced by hMSCs after 72 h transfection of hMSCs. Secreted BMP-2 was found both in medium and on mineral coating (C) BMP-2 detected in the cell culture medium after 72 h transfection of hMSCs by ELISA; only a small portion of secreted BMP-2 was found in medium. (D) BMP-2 detected by dissolving the mineral coating with 200 µL 100 mM EDTA in PBS after 72 h transfection of hMSC by ELISA. The majority of secreted BMP-2 was found in the dissolved mineral coating. # indicates significant differences compared to Lipo2000 * indicates significant differences compared to Lipo2000.